Models of Plasma Processes in Electrostatic Ion Thrusters

Ira Katz
Supervisor, Advanced Propulsion Technology Group
Jet Propulsion Laboratory, California Institute of Technology

American Physical Society 46th Annual Meeting of the Division of Plasma Physics
Plasma Propulsion Mini-Conference

November 18-19, 2004
Savannah, GA

Models of Plasma Processes in Electrostatic Ion Thrusters

- JPL Models of Ion Thruster Physics
  - Motivation
  - Background
  - Approach
    - Basic physical models of plasma processes closely tied to detailed diagnostic experiments (D. Goebel – earlier paper)
    - Separate models of different regions (thruster components)
    - Fluid models whenever possible, limited use of PIC and MC
      - Mostly classical transport coefficients
  - Models
    - Ion optics
    - Hollow cathode insert region
    - Discharge chamber (R. Wirz – following paper)
  - Closely tied to detailed diagnostic experiments (D. Goebel – earlier paper)
- Ion Optics Model Physics
- Hollow Cathode Insert Region Physics

Electric Propulsion at JPL

Vision: "***Advanced Electric Propulsion for NASA's Science Spacecraft***"

flight project

project planning

EP mission assurance

technology for missions

advanced technology

Roles and Resources

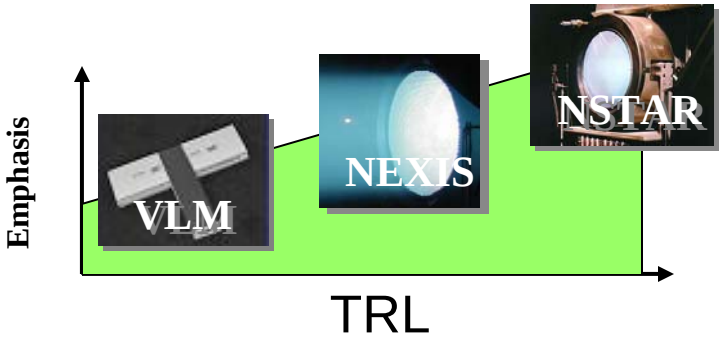

Wide Range of Technology Development Guided by Flight Project Needs

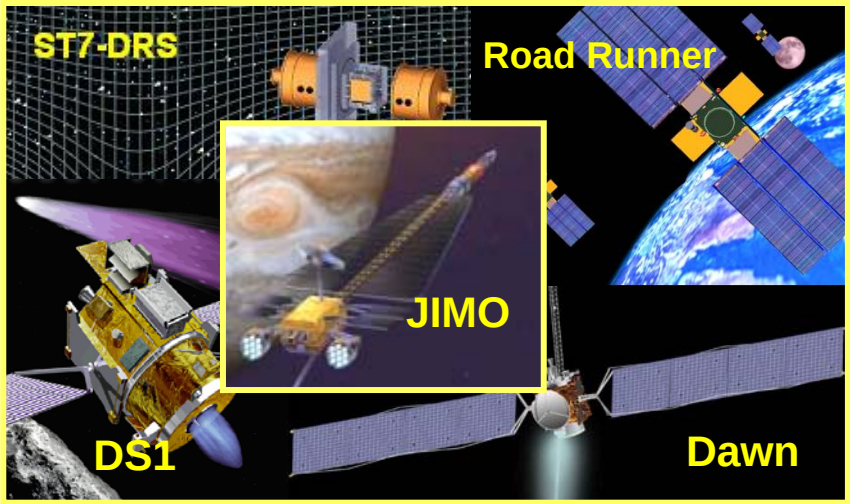

Flight Project Experience

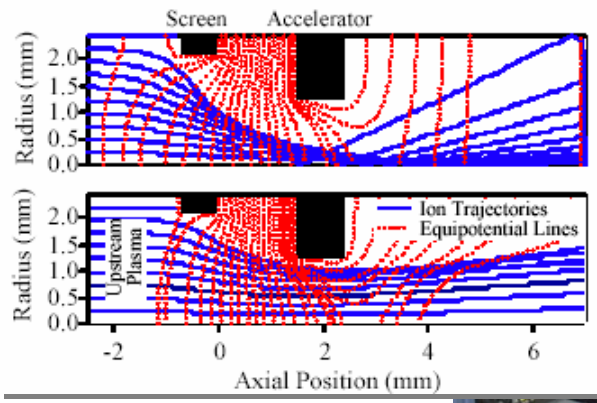

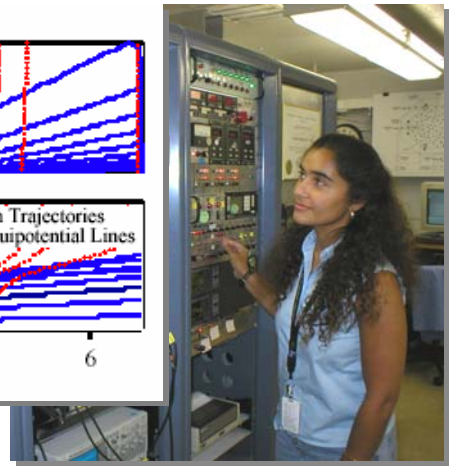

Focus on Understanding Basic Processes: Coordinated Modeling & Experiment

Ion Thruster Fundamentals

1. Xenon gas **ionized** in the discharge chamber
2. Ion **accelerated** electric field between grids
3. Ion beam charge and current **neutralized** by neutralizer electrons

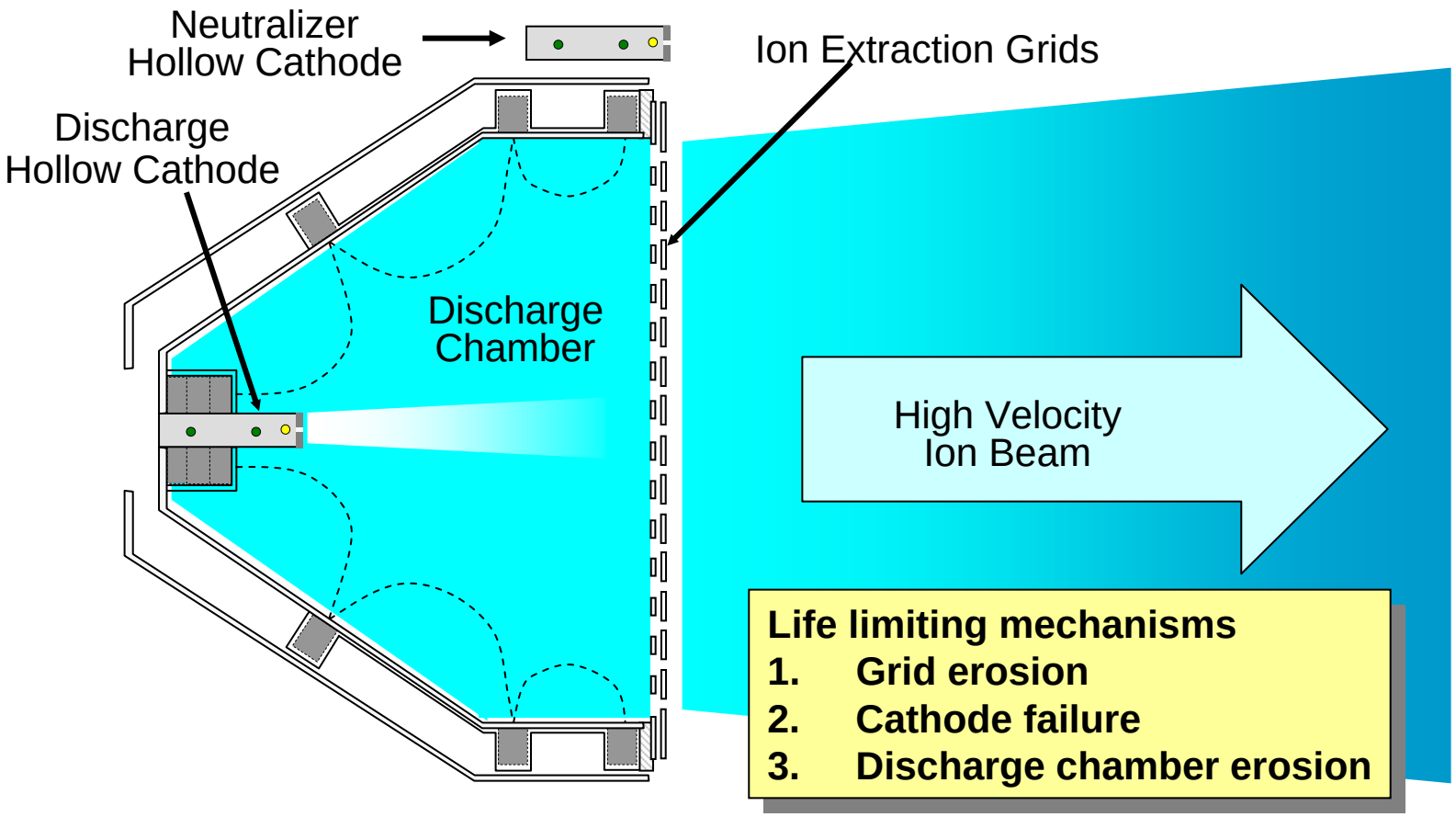

JPL Computer Models Will Address All Aspects of Ion Thruster Physics

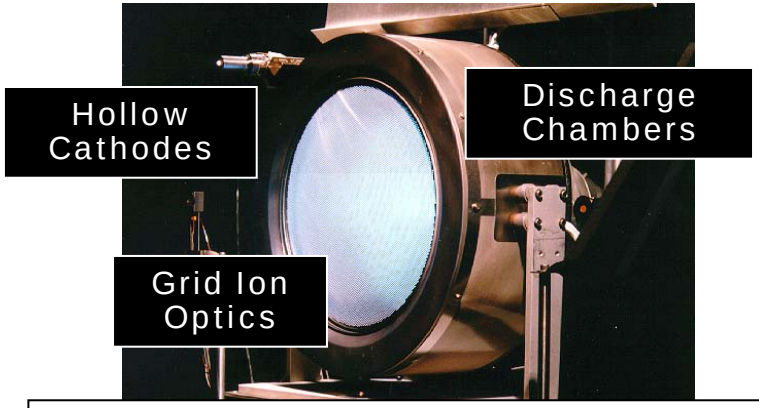

Computer models are used to guide design, correlate test data & predict engine life
Validated with lab & flight performance & wear data

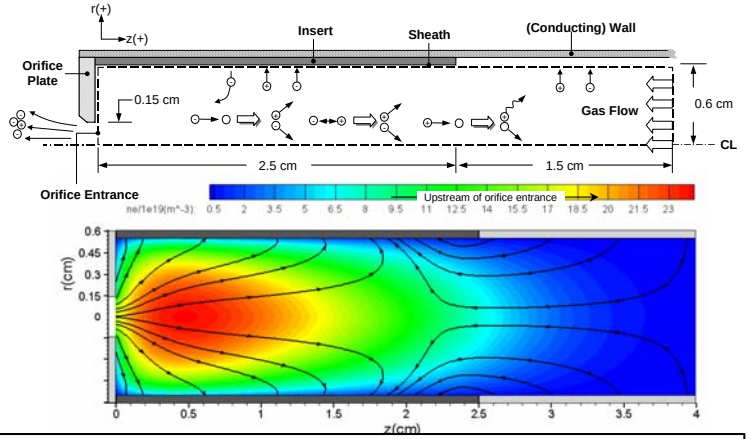

Hollow cathode orifice and discharge chamber models include ionization physics

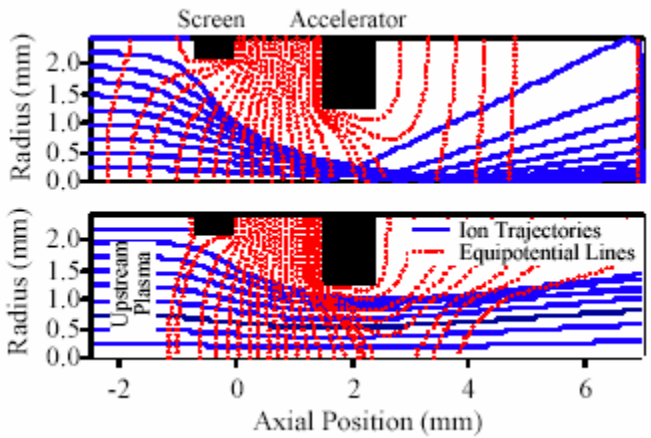

ion trajectories

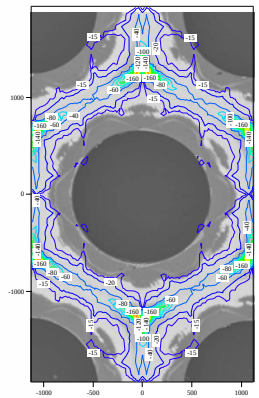

erosion pattern

Codes model ion trajectories and erosion of a single grid aperture

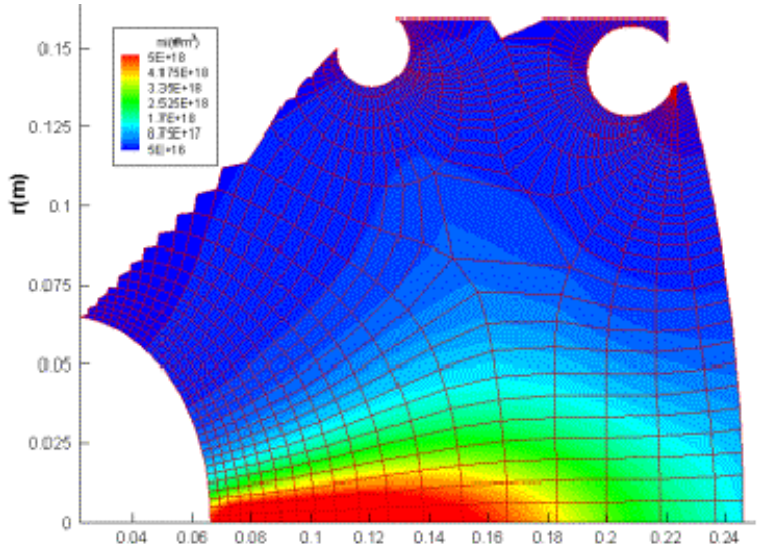

Discharge chamber plasma densities

Approach to Understanding Life Limiting Mechanisms in Hollow Cathodes at JPL

- Theoretical models <u>alone not sufficient</u>
  - Simplified (0-D, 1-D) models do not provide the required quantitative insight on life limiting physics
  - Comprehensive 2-D models require validation and information on boundary conditions

- Experiments <u>alone not sufficient</u>
  - Access to off-axis regions difficult
  - Dependence of all pertinent quantities (e.g. fluxes to walls) on operating conditions can not be identified by empirical means alone
  - Proposed launch date for JIMO (2015) does not allow sufficient time to demonstrate HC life in the lab

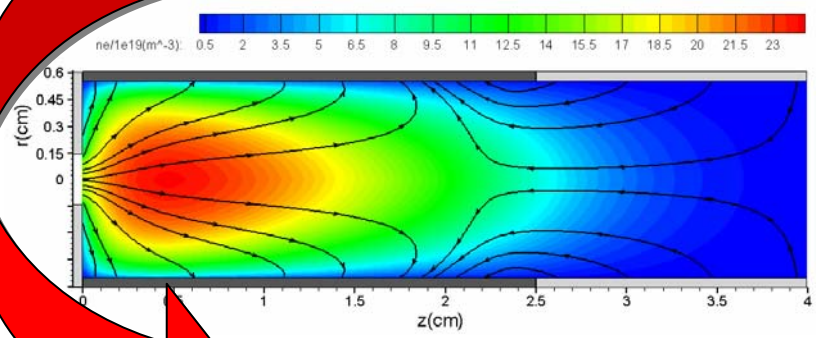

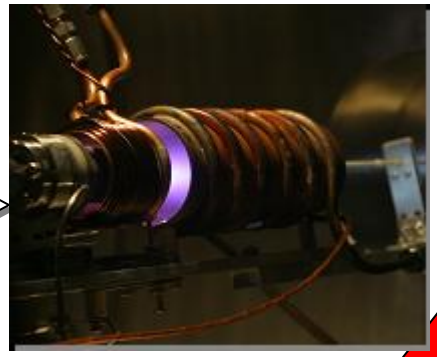

Focused effort that combines experiment with detailed theoretical modeling to assess life limiting mechanisms

Maxwellian Electron Charge

Introduces Non-linear Terms in the Potential

$$\nabla^2\phi = -\frac{\rho}{\varepsilon_0} = -\frac{e}{\varepsilon_0}(n_i - n_e)$$

$$n_e(\phi) = n_{ref}\exp((\phi - \phi_{ref})/\theta_{ref})$$

$$\frac{\partial n}{\partial \phi} = \frac{n_e}{\theta_{ref}}$$

$$\nabla^2\phi \approx -\frac{e}{\varepsilon_0}\left(n_i - n_e(\phi_0) - \frac{n_e(\phi_0)}{\theta_{ref}}(\phi - \phi_0)\right)$$

Code iterates on linearized equations

```
Nonlinear terms in Matgen (only for diagonal tems of non fixed potentials)
    nePhi0=neRef(j)*exp((phi(i,j)-phiRef(j))/TeRef(j))
    aa(ij)=c(i)+cellVol(i)*(e/e0)*nePhi0/TeRef(j)
    bb(ij)=-q(i,j)/e0 + cellVol(i)*(e/e0)*nePhi0*phi(i,j)/TeRef(j)
```

Two-Grid Ion Optics System Aperture Pairs

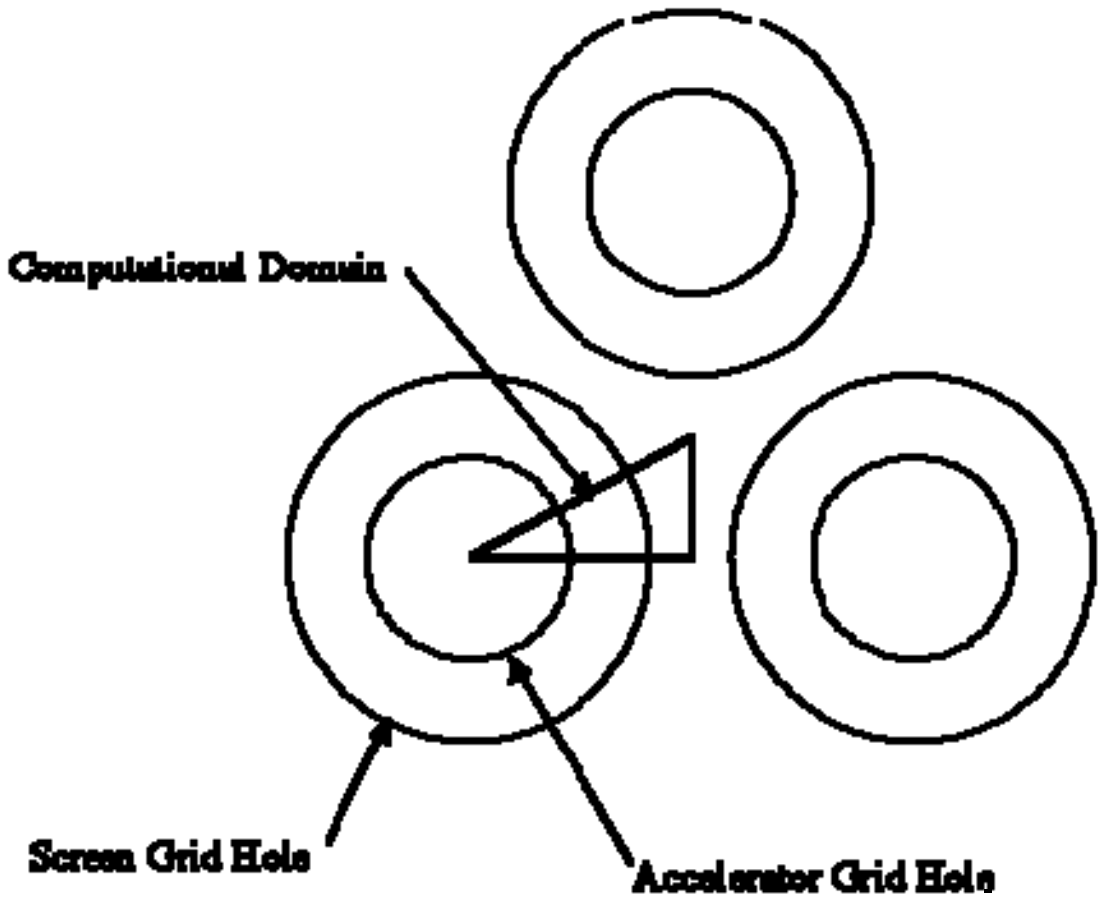

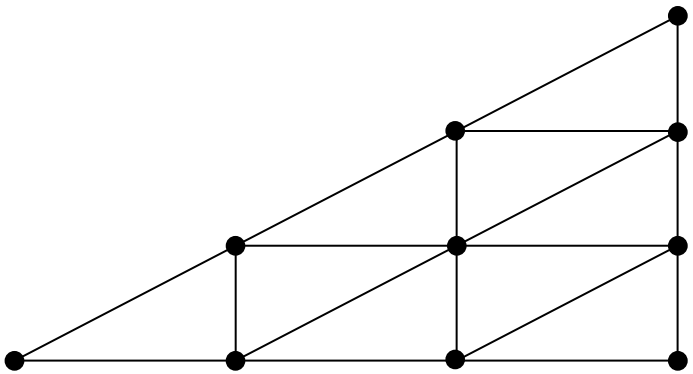

NSTAR Accelerator Grid

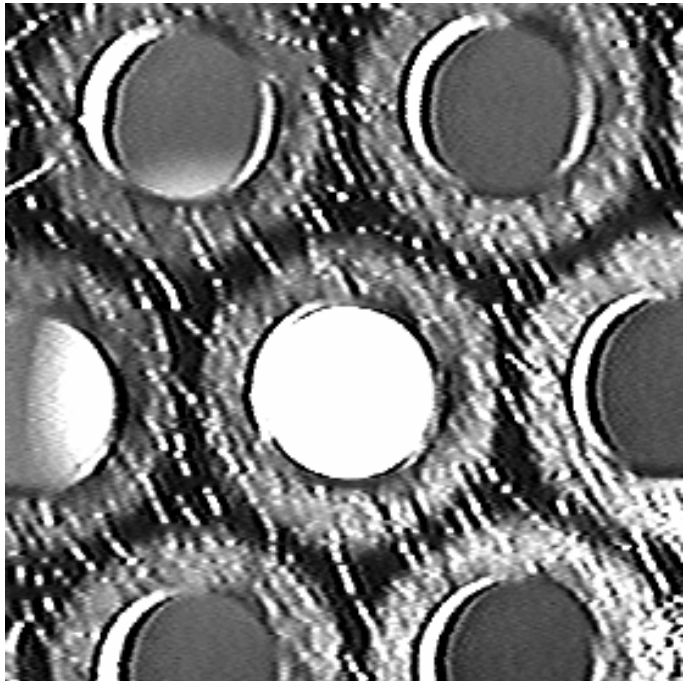

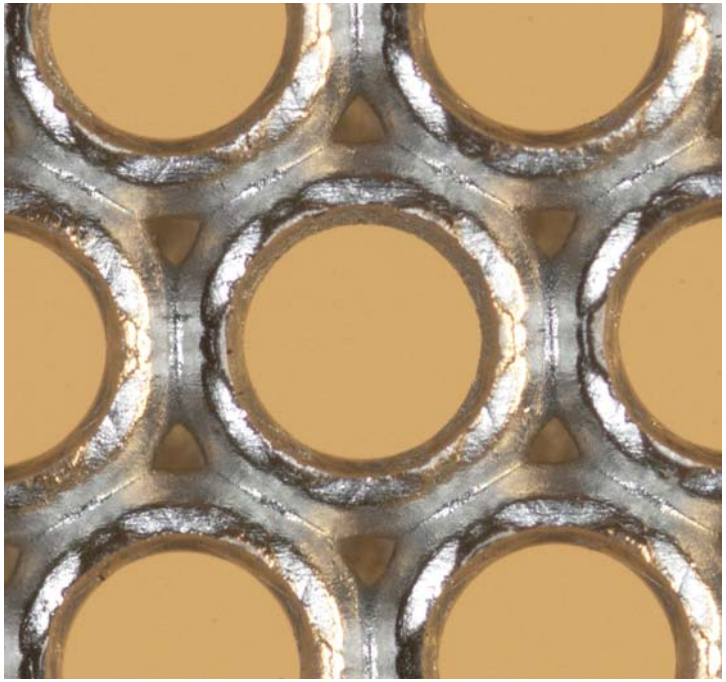

NSTAR thruster accelerator grid at 125 hours (left) and 30,352 hours (right)

CEX3D Wear Pattern Prediction for NSTAR Thruster

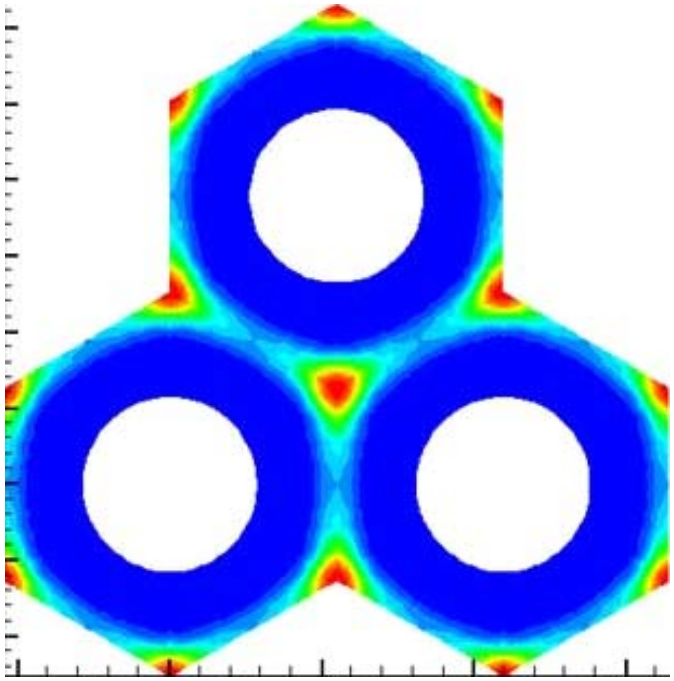

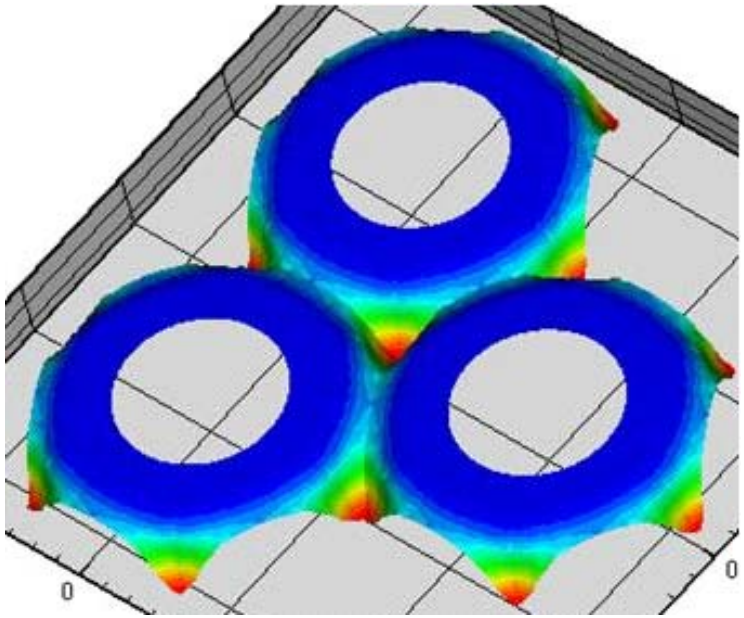

Basic Setup and Plasma Parameters for Hollow Cathode Insert Region Under Study

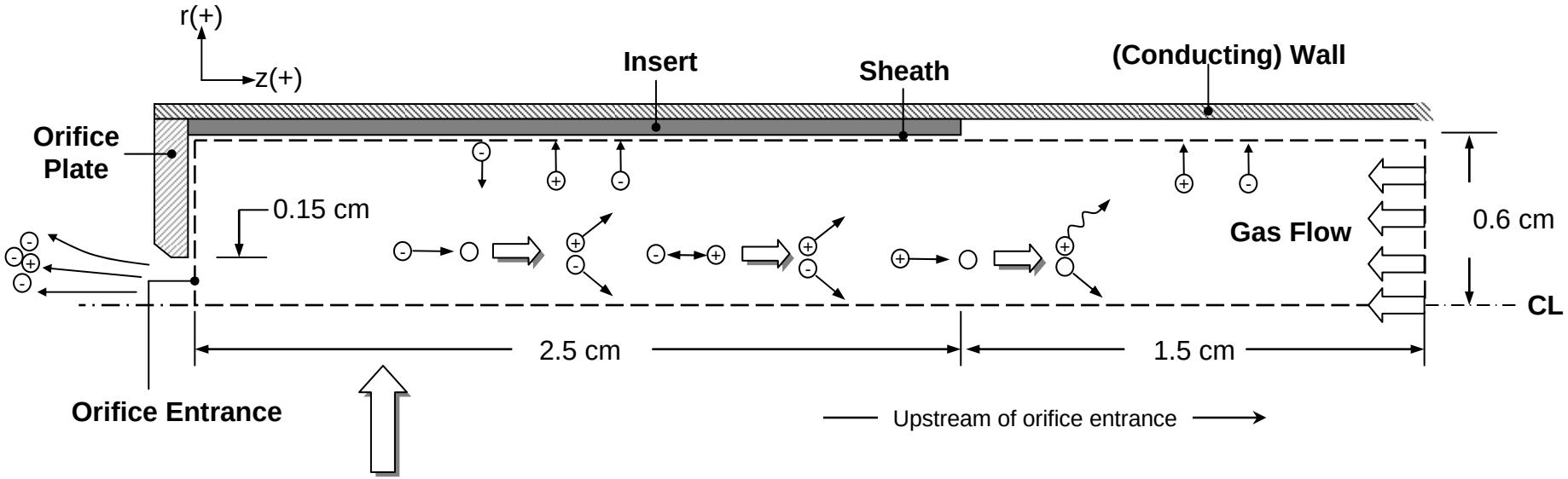

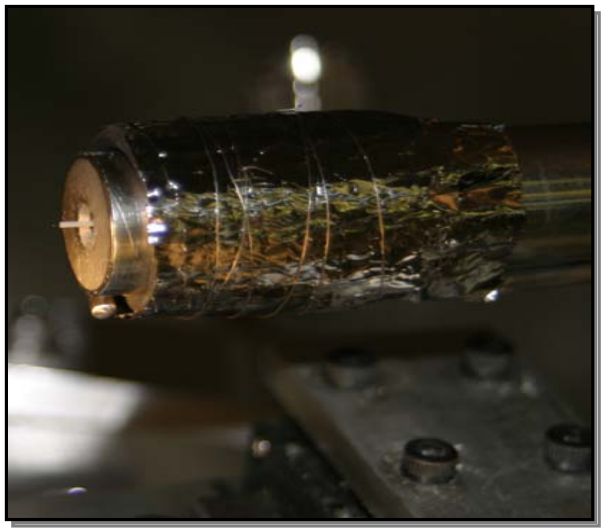

Nominal operating condition for HC under study:

Orifice Entrance $n=5e19 m^{-3}$, $T_e=2eV$, $n_n=5e21\ m^{-3}$, $T=3000\ ^\circ K$, $\bar{u}_n=5\ m/s$	Dense Plasma Region $n=2e20 m^{-3}$, $T_e=1.8eV$ $n_n=3e21\ m^{-3}$, $T=3600\ ^\circ K$, $\bar{u}_n=5\ m/s$
$\nu_{en}^{-1}=1.7e\text{-}9\ s$, $\lambda_{en} \approx 1.0\ mm$	$\nu_{en}^{-1}=3.3e\text{-}9\ s$, $\lambda_{en} \approx 1.85\ mm$
$\nu_{ei}^{-1}=2.4e\text{-}9\ s$, $\lambda_{ei} \approx 1.4\ mm$	$\nu_{ei}^{-1}=0.56e\text{-}9\ s$, $\lambda_{ei} \approx 0.32\ mm$
$\nu_{in}^{-1}=2.9e\text{-}7\ s$, $\lambda_{in} \approx 0.2\ mm$	$\nu_{in}^{-1}=4.4e\text{-}7\ s$, $\lambda_{in} \approx 0.33\ mm$
$\nu_{iz}^{-1}=1.7e\text{-}6\ s$, $\lambda_{iz} \approx 0.09\ mm$	$\nu_{iz}^{-1}=6.1e\text{-}6\ s$, $\lambda_{iz} \approx 0.031\ mm$
$\omega_b^{-1}=1.7e\text{-}9\ s$, $\omega_b(\nu_{en}+\nu_{ei})^{-1}=0.58$	$\omega_b^{-1}=9.0e\text{-}8\ s$, $\omega_b(\nu_{en}+\nu_{ei})^{-1}=0.005$

2½-D Hollow Cathode Insert Plasma Model

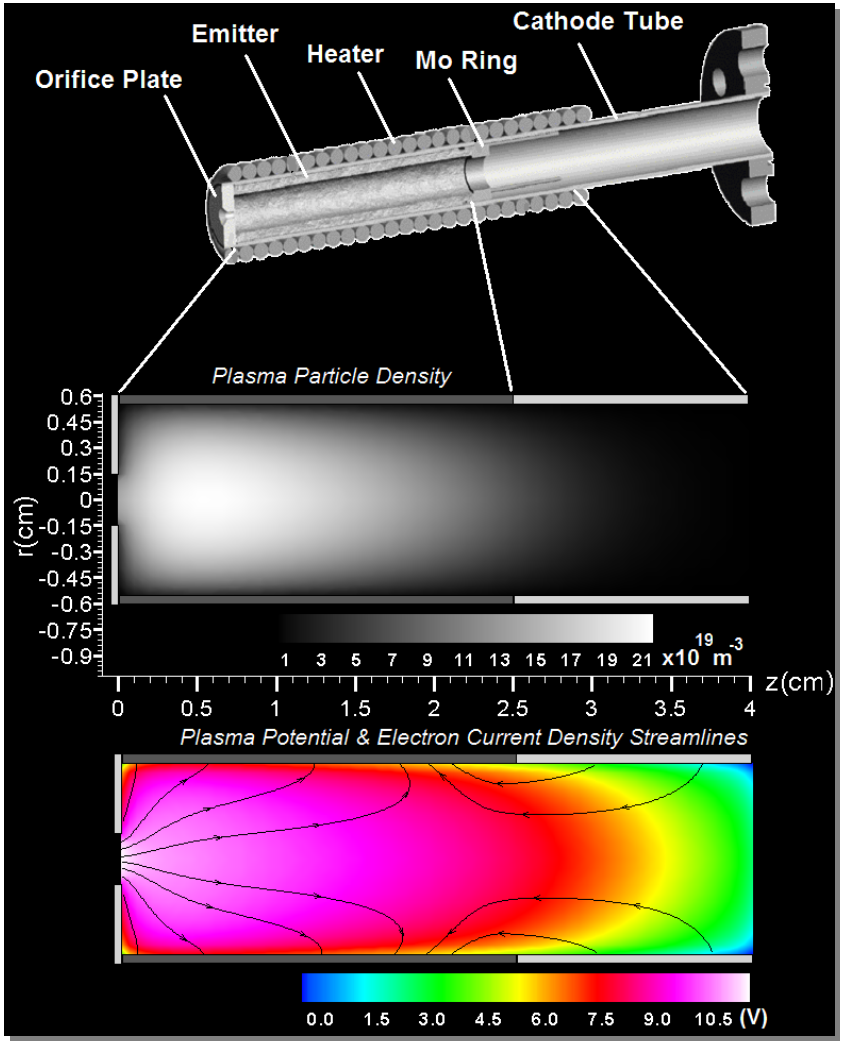

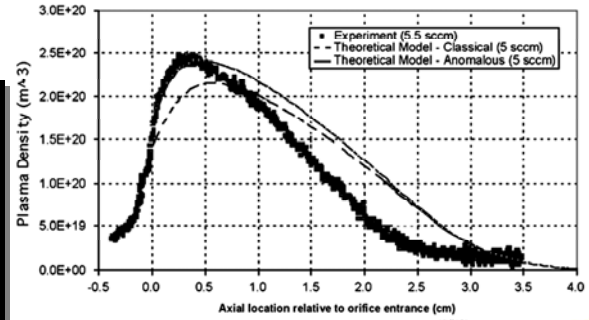

Plasma density comparisons

Plasma potential and Te comparisons

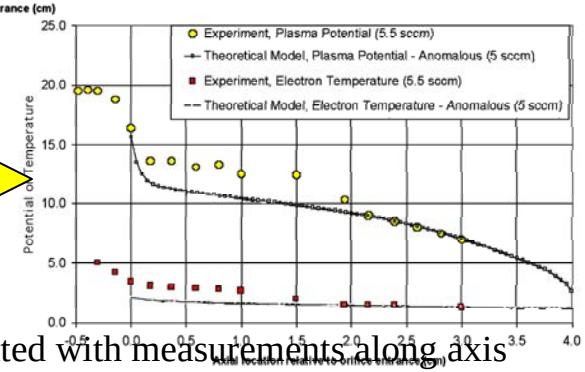

- Plasma model validated with measurements along axis
- Close to emitter model calculates:
  - Potential drop <≈ 8V
  - Ion flux <≈ 1 A/cm^2 (6x10^{18}/cm^2/sec)

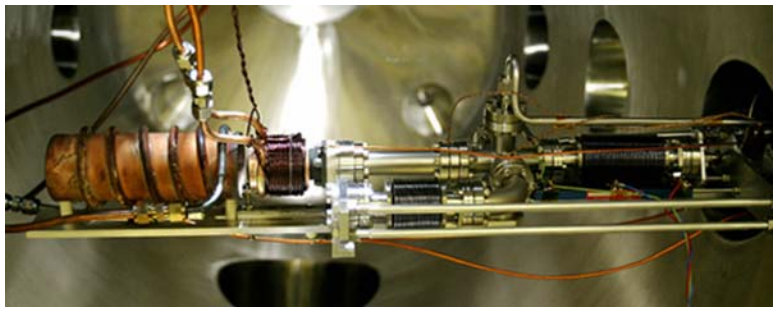

Hollow Cathode Insert Region Model
- Governing Equations for Plasma -

Combined Steady-State Momentum Equations for Plasma Species with no Inertia

$$ne\mathbf{E} \approx -\nabla p_e - \mathbf{R}_{ei} - nm_e\nu_{en}\mathbf{u}_e$$

$$-ne\mathbf{E} \approx -\nabla p_i - \mathbf{R}_{ie} - nm_i\nu_{in}\mathbf{u}_i$$

$$+ \longrightarrow n\mathbf{u}_i = \frac{e}{m_i\nu_{in}(1+\nu)}\left[\frac{m_e\nu_{en}}{e^2}\mathbf{j}_e - \nabla(nT_i + nT_e)\right], \quad \nu \equiv \frac{\nu_{iz}}{\nu_{in}}$$

Ion Continuity Equation

$$\frac{\partial n}{\partial t} + \nabla\cdot(n\mathbf{u}_i) - \nu_{iz}n = 0$$

$\Rightarrow$ n

Energy Transport Equation for Electrons

$$\frac{\partial}{\partial t}\left(\frac{3}{2}neT_e\right) = \nabla\cdot\left(\frac{5}{2}T_e\mathbf{j}_e + \kappa_e\nabla T_e\right) + \mathbf{E}\cdot\mathbf{j}_e - 3n\frac{m_e}{m}(\nu_{ei}+\nu_{en})(T_e - T) - \dot{n}e\varepsilon_i$$

$\Rightarrow$ T_e

Steady-State Mass Conservation

$$\nabla\cdot(\mathbf{j}_e + \mathbf{j}_i) = \nabla\cdot\left[\frac{\nabla(nT_e)}{(\eta_{cl}+\eta_{anom})n} - \frac{\nabla\phi}{(\eta_{cl}+\eta_{anom})} + \mathbf{j}_i\left(1 - \frac{\nu_{ei}}{\nu_{en}+\nu_{ei}}\right)\right] = 0$$

$\Rightarrow$ $\phi, \mathbf{E}$

$$\eta_{cl} \equiv \frac{m_e(\nu_{en}+\nu_{ei})}{ne^2}, \quad \eta_{anom} \equiv \frac{m_e\nu_{anom}}{ne^2}$$

Hollow Cathode Insert Region Model
- Governing Equations for Heavy Species -

Energy Transport Equation for Heavy Species "s"

$$\frac{\partial}{\partial t}\left(\frac{3}{2}p_s\right)+\nabla\cdot\left(\frac{5}{2}p_s\mathbf{u}_s+\mathbf{q}_s\right)-\mathbf{u}_s\cdot\nabla p_s=Q_s$$

Ions (s=i)

$$\frac{\partial}{\partial t}\left(\frac{3}{2}p_i\right)+\nabla\cdot\left[\frac{5}{2}p_i\mathbf{u}_i+\mathbf{q}_i\right]-\mathbf{u}_i\cdot\nabla p_i=Q_i$$

Neutrals (s=n)

$$\frac{\partial}{\partial t}\left(\frac{3}{2}p_n\right)+\nabla\cdot\left[\frac{5}{2}p_n\mathbf{u}_n+\mathbf{q}_n\right]-\mathbf{u}_n\cdot\nabla p_n=Q_n$$

(+)

$$T_i=T_n=T,\ \ n_n+n\approx n_n,\ \nabla p\approx 0,\ \mathbf{u}_n\approx 0,\ \kappa_n>>\kappa_i$$

$$\frac{\partial}{\partial t}\left(\frac{3}{2}n_nkT\right)+\nabla\cdot\left[\frac{5}{2}nkT\mathbf{u}_i-\kappa_n\nabla T\right]-\mathbf{u}_i\cdot\nabla nkT\approx Q_i+Q_n$$

$$Q_i+Q_n\approx nm\nu_{in}u_i^{\,2}+3\frac{m_e}{m}nk\left(\nu_{ei}+\nu_{en}\right)\left(T_e-T\right)$$

$\Rightarrow$ T

$$p=p_n+p_i+p_e\Rightarrow n_n=\frac{p}{kT}-n\left(1+\frac{T_e}{T}\right)$$

$\Rightarrow$ n_n

Anomalous Effects and Turbulent Heating of the Plasma in the Insert Region

2-stream Stability Diagram (Stringer, 1964)

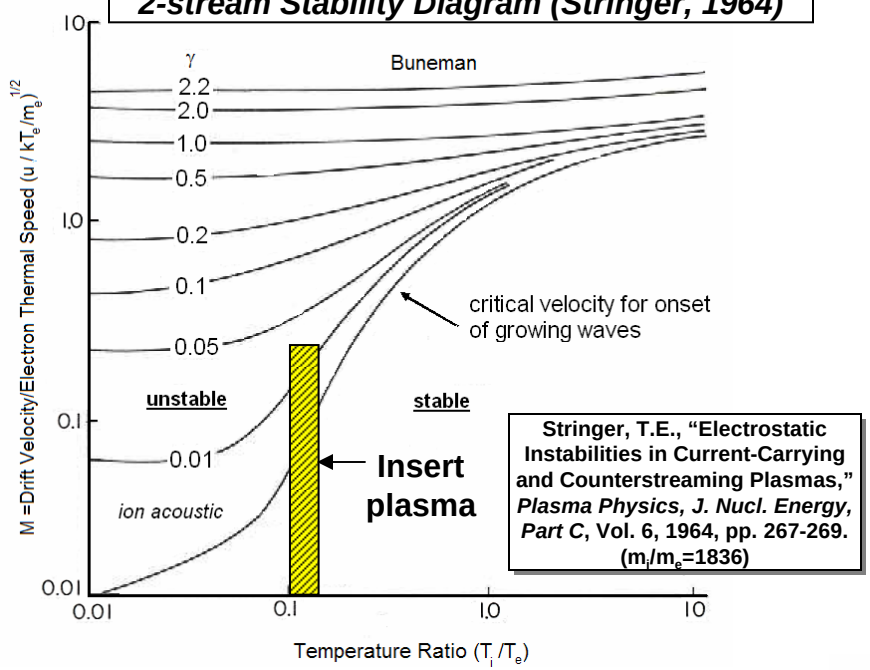

Stringer, T.E., "Electrostatic Instabilities in Current-Carrying and Counterstreaming Plasmas," *Plasma Physics, J. Nucl. Energy, Part C*, Vol. 6, 1964, pp. 267-269. (m_i/m_e=1836)

Computed profiles along CL for 25 A, 5sccm case

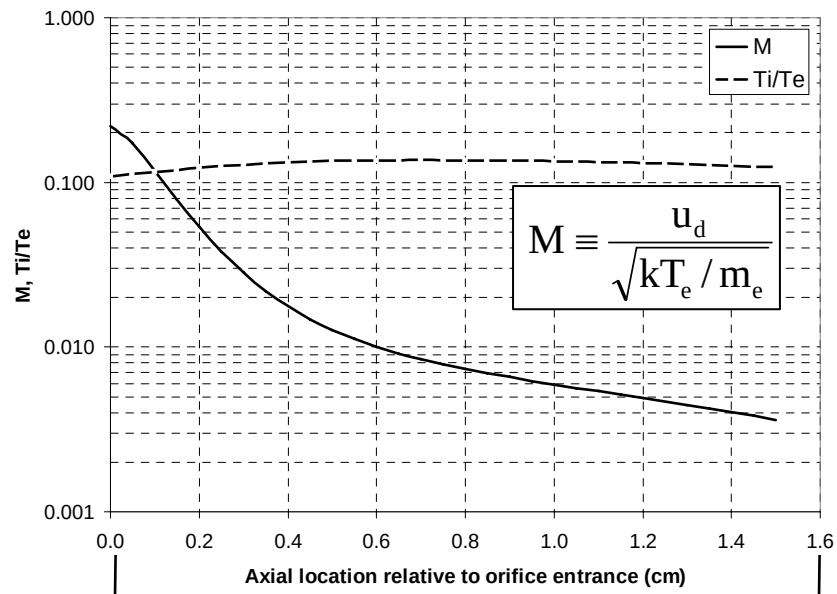

$$M \equiv \frac{u_d}{\sqrt{kT_e / m_e}}$$

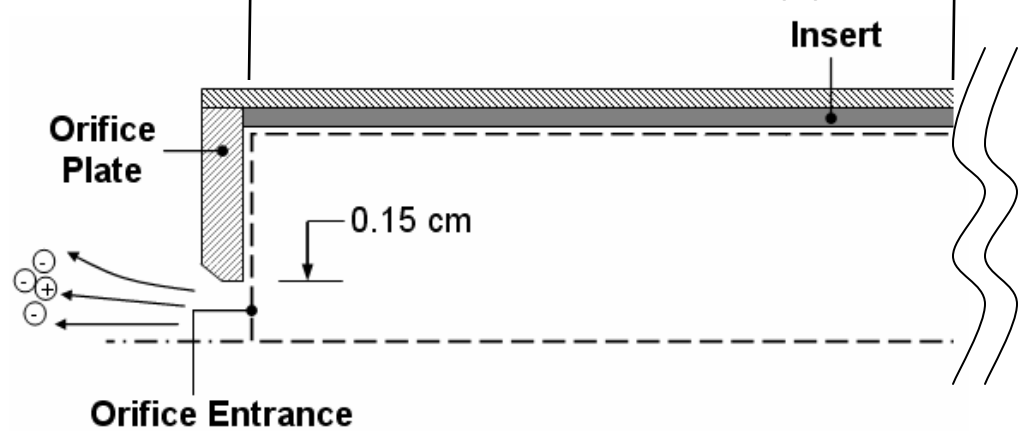

Sagdeev, R.Z. (1967)

$$u_e > u_d > \sqrt{kT_e / m_i}$$

$$\rightarrow \nu_{anom} \approx 10^{-2} \frac{T_e}{T_i} \frac{u_d}{\sqrt{kT_e / m_e}} \omega_{pe}$$

Results and Comparisons with Measurements, I

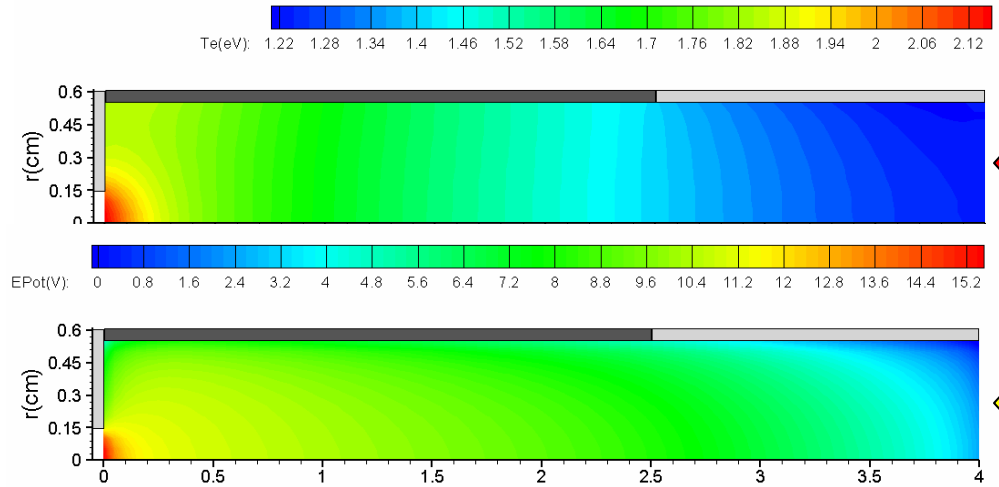

Electron Temperature (Anomalous model)

Plasma potential (Anomalous model)

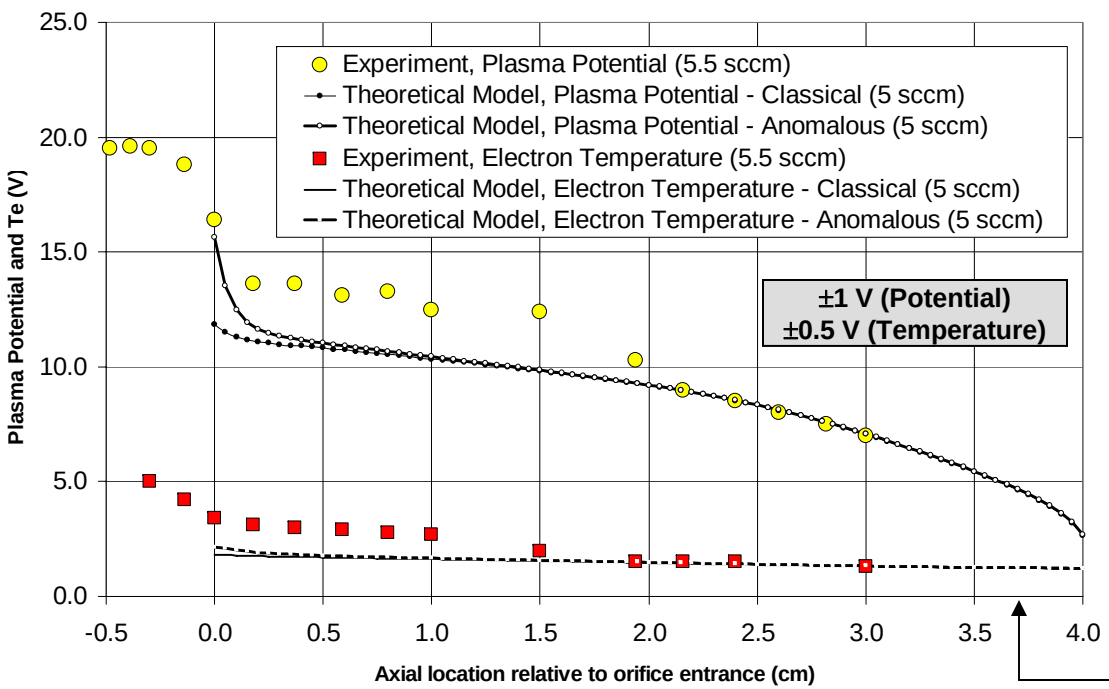

- Excellent agreement between computed and measured values upstream of orifice → Classical transport. Turbulent heating possible near orifice.
- Maximum discrepancy on T_e occurs at orifice entrance (less than a factor of 2).
- T_e < 1.85 eV near insert wall
- ϕ < 8V near insert wall

Profiles along C_L

Results and Comparisons with Measurements, **II**

Plasma Density and Electron Current Density Streamlines

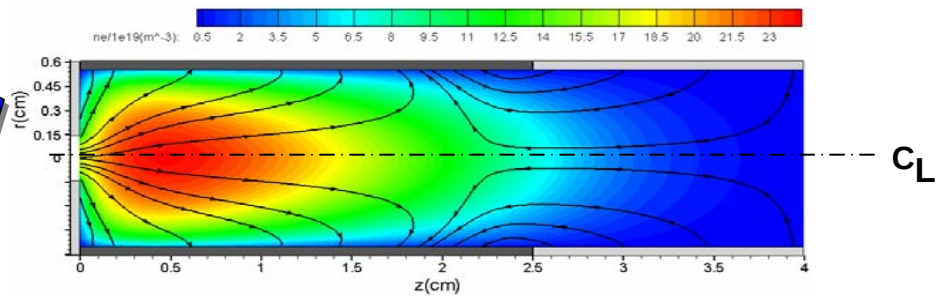

Different density profiles at similar flow rates suggest change in insert emission characteristics after a few hundred hours of operation

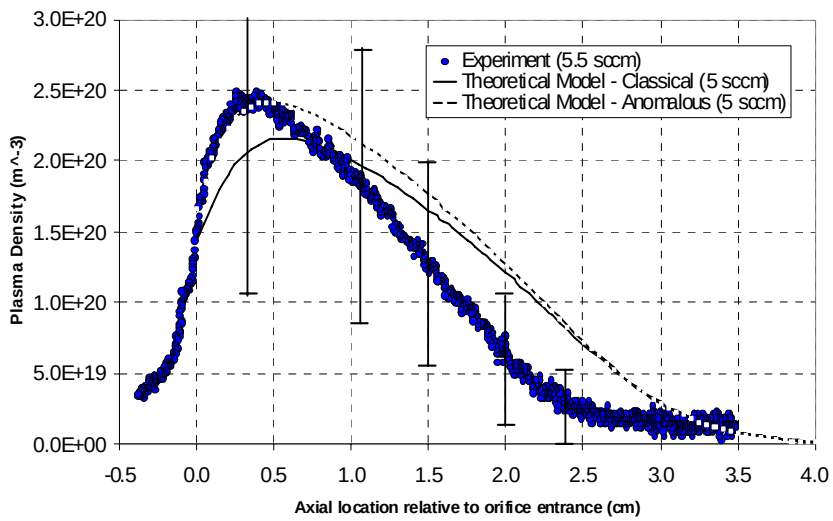

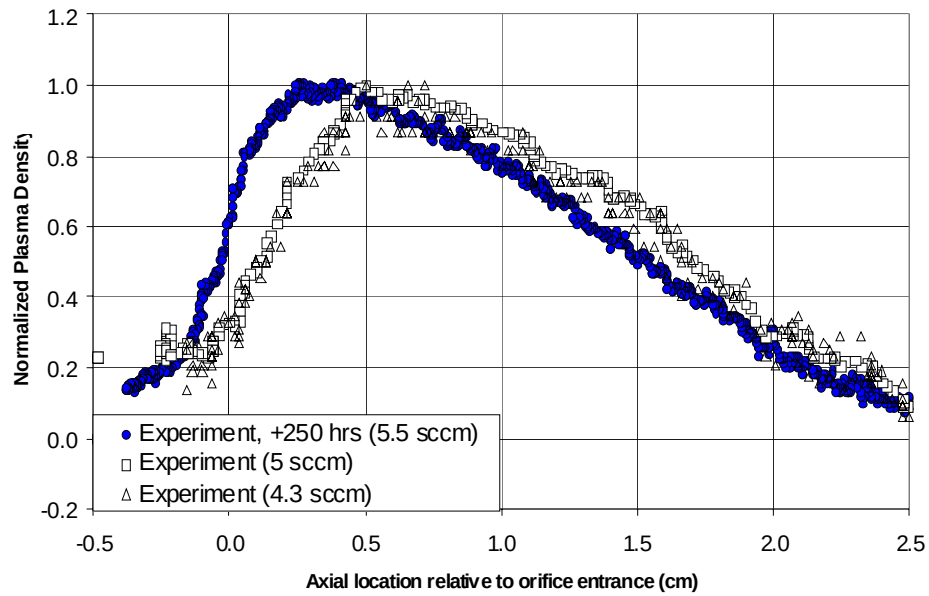

Profiles along C_L

…And More Results

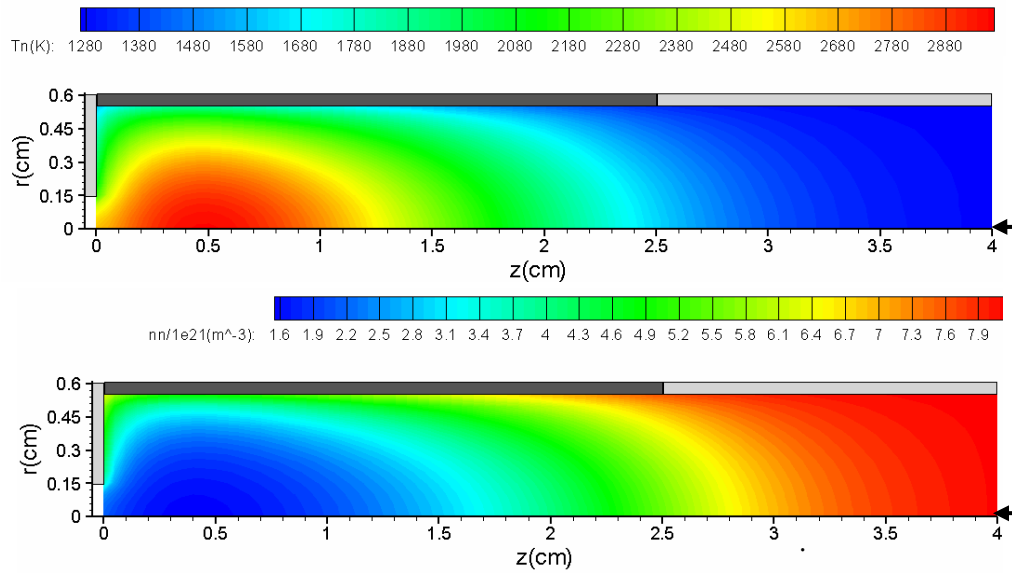

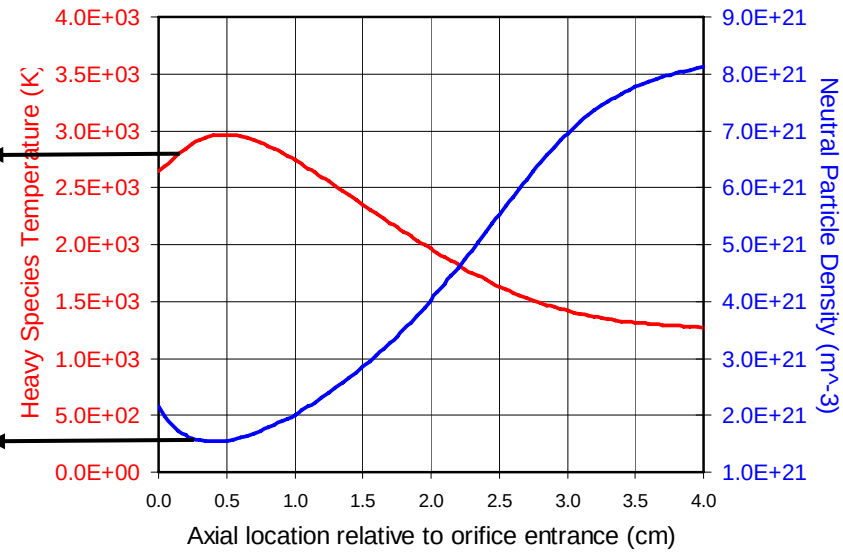

Power distribution in the insert region

Site	Source	(W)
Input Power and Work by Electric Field		
Insert	Emitted e-	262.2
Plasma	Electric field ($\mathbf{E}\cdot\mathbf{j}_e$)	111.2
Output Power and Losses		
Insert	Absorbed e-	138.0
Conductive Wall	Absorbed e-	11.8
Orifice Plate	Absorbed e-	23.6
Orifice	Out-flowing e-	133.3
Plasma	Ionization	65.1
Plasma	Thermal Equilibration	1.6

Currents to Surfaces

$$I_s = \iint_A \mathbf{j}_s \cdot (\hat{\mathbf{n}} dA)$$

Site	Emitted (A)		Absorbed (A)	
Orifice Plate	$I_e = 0.0$	$I_i = 0.0$	$I_e = -2.09$	$I_i = 0.81$
Insert Wall (Emitter)	$I_e = 37.6$	$I_i = 0.0$	$I_e = -13.4$	$I_i = 4.39$
Conductive Wall	$I_e = 0.0$	$I_i = 0.0$	$I_e = -2.08$	$I_i = 0.15$
Orifice Entrance	$I_e = -25.0$	$I_i = 0.007$		